Steel and Composite Structures, *Vol. 32, No. 4* (*2019*) *423-441*
DOI: https://doi.org/10.12989/scs.2019.32.4.423

Application of FEM on first ply failure of composite hypar shells with various edge conditions

Arghya Ghosh* and Dipankar Chakravorty [a]

Department of Civil Engineering, *Jadavpur University*, *Kolkata-700032*, *India*

(*Received March 2, 2018, Revised March 21, 2019, Accepted July 31, 2019*)

Abstract. This study aims to accurately predict the first ply failure loads of laminated composite hypar shell roofs with different boundary conditions. The geometrically nonlinear finite element method (FEM) is used to analyse different symmetric and anti-symmetric, cross and angle ply shells. The first ply failure loads are obtained through different well-established failure criteria including Puck's criterion along with the serviceability criterion of deflection. The close agreement of the published and present results for different validation problems proves the correctness of the finite element model used in the present study. The effects of edge conditions on first ply failure behavior are discussed critically from practical engineering point of view. Factor of safety values and failure zones are also reported to suggest design and non-destructive monitoring guidelines to practicing engineers. Apart from these, the present study indicates the rank wise relative performances of different shell options. The study establishes that the angle ply laminates in general perform better than the cross ply ones. Among the stacking sequences considered here, three layered symmetric angle ply laminates offer the highest first ply failure load. The probable failure zones on the different shell surfaces, identified in this paper, are the areas where non-destructive health monitoring may be restricted to. The contributions made through this paper are expected to serve as important design aids to engineers engaged in composite hypar shell design and construction.

Keywords: composite; finite element method (FEM); hypar shell roofs; first ply failure; nonlinear analysis

1. Introduction

Among different advanced structural materials, light weight laminated composites have gained wide popularity in civil and other weight sensitive engineering applications from the second half of the last century due to their design versatility and high stiffness-to-weight and strength-to-weight ratios. To utilize the composites in fabricating civil engineering shell roofing units and also to arrive at safe and economical design, the designer must be aware of the different limitations of the materials for which the failure characteristics are to be studied. Among the different shell configurations used as roofing units, the hyperbolic paraboloidal shell bounded by straight edges (commonly called a hypar shell as shown in Fig. 1(a)) has the special advantage of aesthetic elegance and this form also offers ease in fabrication being doubly ruled surface. In practice, roofs may have different combinations of boundary conditions and a comprehensive study of failure characteristics of this shell with different edge restraints is a prerequisite for using these forms efficiently.

The composites subjected to static overloading may undergo large deflection at the onset of failure and hence the geometrically nonlinear strains are important to be considered. Using the nonlinear strains, a progressive failure algorithm was proposed by Reddy *et al*. (1995) to report the first and ultimate ply failure of laminated composite plates. Singh and Kumar (1998) studied post buckling failure behaviour and progressive failure of thin simply supported symmetric rectangular laminates subjected to in-plane shear loads. Reinoso and Blázquez (2016) reported the post buckling failure responses of composite cylindrical stiffened panels subjected to uniform pressure load using geometric nonlinearity. A theoretical study on multiple failures of in-plane loaded composite laminates containing a through-width delamination was carried out by Xue *et al*. (2019). Xue *et al*. (2017) also presented a multiscale approach to study the nonlinear vibration of fiber reinforced composite laminates containing an embedded, through-width delamination. Pal and Ray (2002) and Prusty (2005) examined the progressive failure behaviour of laminated composite plates and composite stiffened and unstiffened panels respectively. Kelly and Hallström (2005) studied experimentally and numerically the behaviour of laminated composites subjected to transverse loads. Progressive failure of tapered laminated composite plates subjected to uniaxial compression was reported by Ganesan and Liu (2008). A progressive failure study of laminated composite plates using Tsai-Wu failure theories was reported by Ellul *et al*. (2014). The ultimate strength analysis of simply supported, rectangular, composite plates under in-plane compressive load was carried out by Yang and Hayman (2015). The authors established an efficient, semi analytical method based on large deflection theory and first order shear deformation

*Corresponding author, M.E., Research Scholar,
E-mail: mghoshbarasat@gmail.com
[a] Ph.D., Professor, E-mail: prof.dipankar@gmail.com

ISSN: 1229-9367 (Print), 1598-6233 (Online)

theory with linear degradation of the material properties. Nali and Carrera (2012) presented different case studies on failure of laminated composite plates corresponding to the different two dimensional popular failure criteria including Hashin's criterion subjected to mono-axial and bi-axial loadings. Using the Hashin's failure criterion, Coelho *et al*. (2015) reported damage initiation of punctured laminated composites under in-plane tension load. Chen et al. (2012, 2014) proposed a finite element model to study progressive failure of laminated composites. The proposed model considered elasto plastic damage including plasticity effects exhibited by composite materials. The authors first developed the model considering in-ply damage only and later modified it to account for delamination damage also. The failure aspects of composite plates of uniform thickness subjected to uniaxial compression and in-plane positive and negative shear loadings were considered in the work of Singh *et al*. (1997, 1998a, b). Xiong *et al*. (2014) also discussed the failure behaviour of sandwich walled cylindrical shells with metallic lattice truss cores and fiber reinforced composite face sheets under uniaxial compression. Chang and Chiang (2010) studied experimentally and theoretically the first ply failure loads of anti-symmetrically built laminated composite plates. The first ply failure study of laminated composites by different well-established failure criteria and comparison between these failure criteria were reported by Kober and Kuhhorn (2012) and Lopez *et al*. (2009). Linear first ply failure loads of laminated composite singly and doubly curved shell panels subjected to static load were suggested by Adali and Cagdas (2011). Reddy and Reddy (1992) used the geometrically nonlinear finite element formulation to study first ply failure of laminated composite plates. The von-Karman nonlinearity was used by the authors to study the linear and nonlinear failure loads for varying thicknesses and boundary conditions of composite plates. A tensor based geometrically nonlinear finite element formulation considering transverse stretching, thus establishing a 3D constitutive relationship, was reported by Arciniega and Reddy (2007). An extension of Karman-Donnell's theory for non-shallow, long cylindrical shells undergoing large deflection was presented by Xue *et al*. (2013). The governing equation was derived by considering the influence of initial curvature of the shell. Bakshi and Chakravorty (2014) reported the first ply failure behaviour of composite cylindrical shells considering geometrically nonlinear strains. The first ply failure stresses of laminated composite plates and cylindrical shell panels with modified Tsai-Wu's and Hashin's failure criteria taken together with nonlinear finite element method were discussed by Chróścielewski *et al*. (2016). A stochastic nonlinear failure analysis of laminated composite plates under compressive transverse loading was reported by Lal *et al*. (2012). This stochastic first ply failure study considering material nonlinearity under hygro thermal environment and different biaxial loadings was used by Gadade *et al*. (2016a, b). Puck's failure criterion was used in these research works. Dong *et al*. (2014) reported the applicability of Puck's failure theory by proposing simple methods for evaluating various parameters required and this failure theory was extended up to three dimensional stress analysis by Matthias and Kröplin (2012). The 3D-version of the Puck's failure criterion was also used in the research work of Reinoso *et al*. (2017) for anisotropic damage model of laminated fiber-reinforced composites. Lee *et al*. (2015) used this Puck's criterion for progressive damage analysis of composite laminates. First ply failure prediction of an internally pressurized shell was carried out by Gohari *et al*. (2015). They studied theoretical and analytical failure loads of unsymmetrically laminated ellipsoidal woven GFRP composite shell. Gohari *et al*. (2012) studied failure of a circular cylindrical thin walled shell made of GFRP composite subjected to static internal and external pressures. Deformation, delamination, shear deformation and micro buckling failure were investigated. Priyadharshani *et al*. (2017) analysed the glass fiber reinforced polymer (GFRP) stiffened composite plates with and without rectangular cutouts under axial, lateral and combined axial and lateral loadings using finite element method. Oterkus *et al*. (2012) proposed a combination of the finite element method and the peri-dynamic theory to predict the initial and final failure loads of a stiffened composite cylindrical panel with a central slot under combined internal pressure and axial tension.

A number of researchers worked on industrially important shells structures like the conoidal, conical and hypar forms and the associated literature may be studied in details to identify the untouched areas. The performances considering deflection, governing force and moment resultants of cross and angle ply conoidal shells with different boundary conditions and lamina stacking sequences were reported by Das and Chakravorty (2007). The authors also investigated the rank wise performances of shell options and proposed a selection guideline to the practicing engineers by giving a relative performance matrix. Again, relative performances of laminated composite conoidal shells under static bending, free and forced vibration responses were studied by Bakshi and Chakravorty (2013) considering geometric linear strains. Dey and Karmakar (2012) studied the dynamic responses under hygrothermal environment and the effect of rotational speeds on free vibration characteristics of delaminated twisted graphite–epoxy cross ply composite conical shells. For this type of shell, the bending characteristics were studied by Bandyopadhyay and Karmakar (2015). The dynamic low velocity impact study and the static responses including the deflections and stresses on composite hypar shells were reported by Neogi *et al*. (2011) and Kumar *et al*. (2013) respectively.

The above review reveals that extensive investigations were carried out on failure analysis of laminated composite plates and cylindrical shells only. Some of the researchers (Das and Chakravorty 2007, Bakshi and Chakravorty 2013, Dey and Karmakar 2012, Bandyopadhyay and Karmakar 2015, Neogi *et al*. 2011, Kumar *et al*. 2013) worked on different structural behaviours of industrially important conoidal, conical and hypar shells but the failure aspects of these shell forms remain totally unattended. Hence, the industrially preferred and aesthetically appealing doubly ruled hypar shell roofs have drawn a special attention from

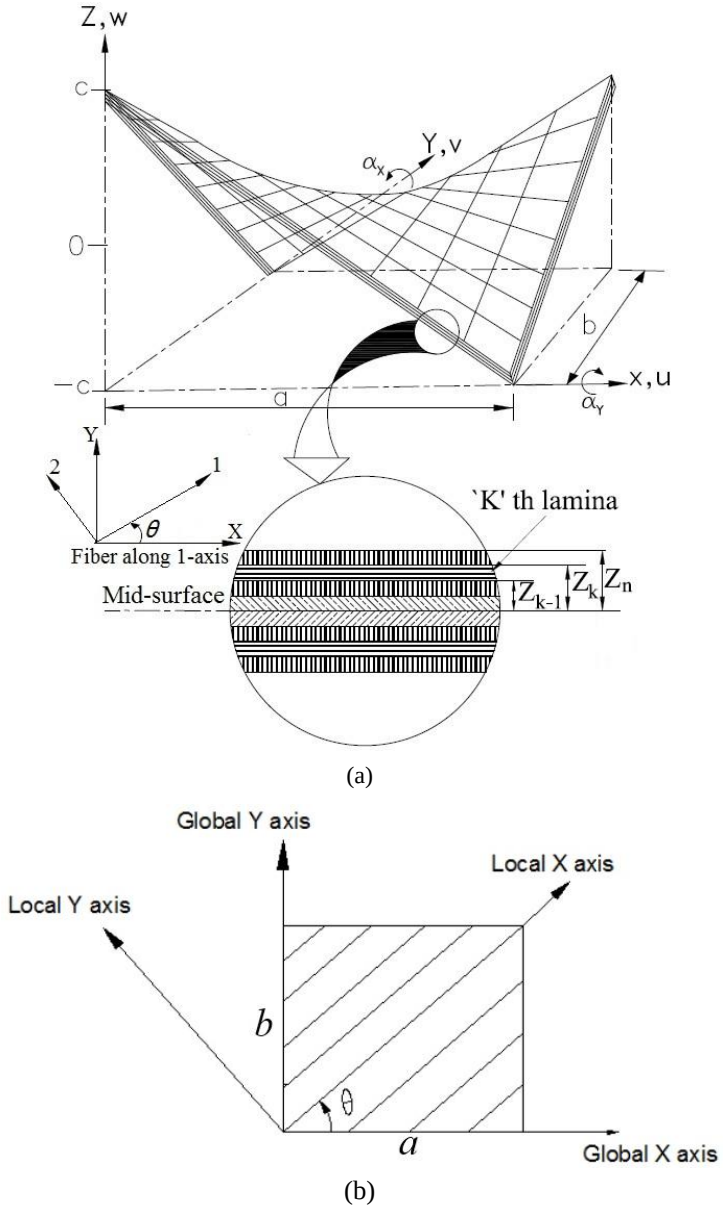

Fig. 1 (a) A typical hypar shell surface; (b) Hypar shell in plan showing fiber orientation of a single lamina

the present authors. In this paper, a finite element method is employed to study the geometrically nonlinear first ply failure behaviour of laminated composite hypar shell roofs with different edge conditions and the results are examined critically from practical point of interest. Though the concept of giving ranks of different shell options in terms of their governing design criteria considering linear strain terms was suggested by earlier researchers (Das and Chakravorty 2007) but such rankings did not consider the criterion of failure probability. The present research focusses on the geometrically nonlinear failure behaviour of composite hypars from practical design angle and also suggests the selection guidelines to the practicing designers for different shell options with various boundary conditions. Laminated composite skewed hypar shells are being investigated recently but only linear failure theories (Ghosh and Chakravorty 2014, 2017) and bending behaviour aspects (Sahoo and Chakravorty 2004) have received attention. Failure study of composite hypar shells using nonlinear strains has been left out totally. The present paper aims to fulfil this lacuna.

2. Mathematical formulation

A laminated composite skewed hypar shell (Figs. 1(a) and (b)) of uniform thickness h and twist radius of curvature R_{xy} is considered. For a given thickness, the shell may consist of any number of thin laminae each of which may be arbitrarily oriented at an angle θ with reference to the X axis of the coordinate system. The surface equation of a typical hypar shell (Sahoo and Chakravorty 2004) is of the form

$$z = \frac{4c}{ab}(x - a/2)(y - b/2) \tag{1}$$

2.1 Finite element formulation

An eight noded isoparametric curved quadratic Serendipity element having five degrees of freedom per node (u, v and w are the displacements along X, Y and Z axes respectively and α_x and α_y are the rotations along X and Y axes respectively) is used for the present skewed hypar shell analysis. The element geometry and the expressions of interpolation functions $[N_i]$ as presented by Owen and Hinton (1980) are used here.

Following Sanders' nonlinear strain-displacement relations and von-Karman type geometric nonlinearity (Reddy 2004), the strain components for a lamina situated at a distance z from the lamina mid-plane of thin shell are evaluated in global axes as

$$\varepsilon_x = \frac{\partial u}{\partial x} + \frac{1}{2}\left(\frac{\partial w}{\partial x}\right)^2 + z\left(\frac{\partial \alpha_x}{\partial x}\right);$$
$$\varepsilon_y = \frac{\partial v}{\partial y} + \frac{1}{2}\left(\frac{\partial w}{\partial y}\right)^2 + z\left(\frac{\partial \alpha_y}{\partial y}\right);$$
$$\gamma_{xy} = \frac{\partial u}{\partial y} + \frac{\partial v}{\partial x} + \frac{2w}{R_{xy}} + \left(\frac{\partial w}{\partial x}\right)\left(\frac{\partial w}{\partial y}\right) + z\left\{\frac{\partial \alpha_x}{\partial y} + \frac{\partial \alpha_y}{\partial x}\right\}; \quad (2)$$
$$\gamma_{xz} = \frac{\partial w}{\partial x} + \alpha_x - \frac{v}{R_{xy}}; \quad \gamma_{yz} = \frac{\partial w}{\partial y} + \alpha_y - \frac{u}{R_{xy}}$$

The generalized strain vector $\{\varepsilon\}$ is expressed by its linear and nonlinear parts as

$$\{\varepsilon\} = \{\varepsilon_l\} + \{\varepsilon_{nl}\} \quad (3)$$

where the nonlinear components of strain are given as

$$\{\varepsilon_{nl}\} = \left\{\frac{1}{2}\left(\frac{\partial w}{\partial x}\right)^2 \;\; \frac{1}{2}\left(\frac{\partial w}{\partial y}\right)^2 \;\; \left(\frac{\partial w}{\partial x}\right)\left(\frac{\partial w}{\partial y}\right)\right\}^T \quad (4)$$

The linear strain field can be expressed in terms of nodal displacements and the resulting relations are

$$\{\varepsilon_l\} = \begin{Bmatrix} \frac{\partial u}{\partial x} \\ \frac{\partial v}{\partial y} \\ \frac{\partial u}{\partial y} + \frac{\partial v}{\partial x} + \frac{2w}{R_{xy}} \\ \frac{\partial \alpha_x}{\partial x} \\ \frac{\partial \alpha_y}{\partial y} \\ \frac{\partial \alpha_x}{\partial y} + \frac{\partial \alpha_y}{\partial x} \\ \frac{\partial w}{\partial x} + \alpha_x - \frac{v}{R_{xy}} \\ \frac{\partial w}{\partial y} + \alpha_y - \frac{u}{R_{xy}} \end{Bmatrix} = \begin{Bmatrix} \frac{\partial \sum N_i u_i}{\partial x} \\ \frac{\partial \sum N_i v_i}{\partial y} \\ \frac{\partial \sum N_i u_i}{\partial y} + \frac{\partial \sum N_i v_i}{\partial x} + \frac{2\sum N_i w_i}{R_{xy}} \\ \frac{\partial \sum N_i \alpha_{xi}}{\partial x} \\ \frac{\partial \sum N_i \alpha_{yi}}{\partial y} \\ \frac{\partial \sum N_i \alpha_{xi}}{\partial y} + \frac{\partial \sum N_i \alpha_{yi}}{\partial x} \\ \frac{\partial \sum N_i w_i}{\partial x} + \sum N_i \alpha_{xi} - \frac{\sum N_i v_i}{R_{xy}} \\ \frac{\partial \sum N_i w_i}{\partial y} + \sum N_i \alpha_{yi} - \frac{\sum N_i u_i}{R_{xy}} \end{Bmatrix}_{i=1\cdots 8}$$
$$= \begin{Bmatrix} \sum \frac{\partial N_i}{\partial x} u_i \\ \sum \frac{\partial N_i}{\partial y} v_i \\ \sum \frac{\partial N_i}{\partial y} u_i + \sum \frac{\partial N_i}{\partial x} v_i + 2\sum \frac{N_i}{R_{xy}} w_i \\ \sum \frac{\partial N_i}{\partial x} \alpha_{xi} \\ \sum \frac{\partial N_i}{\partial y} \alpha_{yi} \\ \sum \frac{\partial N_i}{\partial y} \alpha_{xi} + \sum \frac{\partial N_i}{\partial x} \alpha_{yi} \\ \sum \frac{\partial N_i}{\partial x} w_i + \sum N_i \alpha_{xi} - \sum \frac{N_i}{R_{xy}} v_i \\ \sum \frac{\partial N_i}{\partial y} w_i + \sum N_i \alpha_{yi} - \sum \frac{N_i}{R_{xy}} u_i \end{Bmatrix}_{i=1\cdots 8} \quad (5)$$
$$= \sum \begin{bmatrix} \frac{\partial N_i}{\partial x} & 0 & 0 & 0 & 0 \\ 0 & \frac{\partial N_i}{\partial y} & 0 & 0 & 0 \\ \frac{\partial N_i}{\partial y} & \frac{\partial N_i}{\partial x} & \frac{2N_i}{R_{xy}} & 0 & 0 \\ 0 & 0 & 0 & \frac{\partial N_i}{\partial x} & 0 \\ 0 & 0 & 0 & 0 & \frac{\partial N_i}{\partial y} \\ 0 & 0 & 0 & \frac{\partial N_i}{\partial y} & \frac{\partial N_i}{\partial x} \\ 0 & -\frac{N_i}{R_{xy}} & \frac{\partial N_i}{\partial x} & N_i & 0 \\ -\frac{N_i}{R_{xy}} & 0 & \frac{\partial N_i}{\partial y} & 0 & N_i \end{bmatrix} \begin{Bmatrix} u_i \\ v_i \\ w_i \\ \alpha_{xi} \\ \alpha_{yi} \end{Bmatrix}_{i=1\cdots 8} = [B]\{d_e\}$$

Now, the generalised strain displacement relations are expressed as

$$\{\varepsilon\} = ([B] + 0.5[B'])\{d_e\} \quad (6)$$

where, $[B]$ is the linear part and $[B']$, dependent on displacement, is the nonlinear part of the strain displacement matrix $[\bar{B}]$ and $\{d_e\}$ is the displacement vector.

Now,

$$[\bar{B}] = [B] + [B'] = [B] + [A'][G'] \quad (7)$$

where

$$[A'] = \begin{bmatrix} \frac{\partial w}{\partial x} & 0 & \frac{\partial w}{\partial y} & 0 & 0 & 0 & 0 & 0 \\ 0 & \frac{\partial w}{\partial y} & \frac{\partial w}{\partial x} & 0 & 0 & 0 & 0 & 0 \end{bmatrix}^T$$

and $[G'] = \begin{bmatrix} 0 & 0 & \frac{\partial N_i}{\partial x} & 0 & 0 \\ 0 & 0 & \frac{\partial N_i}{\partial y} & 0 & 0 \end{bmatrix}_{i=1\cdots 8}$

2.2 Lamina constitutive relations

The force and moment resultant vector $\{F\}$ is expressed as

$$\{F\}=\begin{Bmatrix} N_x \\ N_y \\ N_{xy} \\ M_x \\ M_y \\ M_{xy} \\ Q_x \\ Q_y \end{Bmatrix} = \begin{bmatrix} A_{11} & A_{12} & A_{16} & B_{11} & B_{12} & B_{16} & 0 & 0 \\ A_{12} & A_{22} & A_{26} & B_{12} & B_{22} & B_{26} & 0 & 0 \\ A_{16} & A_{26} & A_{66} & B_{16} & B_{26} & B_{66} & 0 & 0 \\ B_{11} & B_{12} & B_{16} & D_{11} & D_{12} & D_{16} & 0 & 0 \\ B_{12} & B_{22} & B_{26} & D_{12} & D_{22} & D_{26} & 0 & 0 \\ B_{16} & B_{26} & B_{66} & D_{16} & D_{26} & D_{66} & 0 & 0 \\ 0 & 0 & 0 & 0 & 0 & 0 & S_{11} & S_{12} \\ 0 & 0 & 0 & 0 & 0 & 0 & S_{12} & S_{22} \end{bmatrix} \begin{Bmatrix} \varepsilon_x^0 \\ \varepsilon_y^0 \\ \gamma_{xy}^0 \\ k_x \\ k_y \\ k_{xy} \\ \gamma_{xz}^0 \\ \gamma_{yz}^0 \end{Bmatrix} = [E]\{\varepsilon\} \tag{8}$$

where

$$\begin{aligned} A_{ij} &= \sum_{k=1}^{np} (Q_{ij})_k (z_k - z_{k-1}); \\ B_{ij} &= \frac{1}{2}\sum_{k=1}^{np} (Q_{ij})_k (z_k^2 - z_{k-1}^2); \\ D_{ij} &= \frac{1}{3}\sum_{k=1}^{np} (Q_{ij})_k (z_k^3 - z_{k-1}^3)... \qquad i, j = 1, 2, 6; \\ S_{ij} &= \sum_{k=1}^{np} F_i F_j (G_{ij})_k (z_k - z_{k-1})... \qquad i, j = 1, 2 \end{aligned} \tag{9}$$

where Q_{ij} are elements of the off-axis elastic constant matrix which is given by

$$[Q_{ij}] = [T]^T \begin{bmatrix} (1-\nu_{12}\nu_{21})^{-1}E_{11} & (1-\nu_{12}\nu_{21})^{-1}E_{11}\nu_{21} & 0 \\ (1-\nu_{12}\nu_{21})^{-1}E_{11}\nu_{21} & (1-\nu_{12}\nu_{21})^{-1}E_{22} & 0 \\ 0 & 0 & G_{12} \end{bmatrix} [T] \tag{10}$$

in which

$$[T] = \begin{bmatrix} \cos^2\theta & \sin^2\theta & \cos\theta\sin\theta \\ \sin^2\theta & \cos^2\theta & -\cos\theta\sin\theta \\ -\sin 2\theta & \sin 2\theta & \cos 2\theta \end{bmatrix}$$

F_i and F_j of Eq. (9) are two factors presently taken as unity for thin shells and

$$[G_{ij}] = \begin{bmatrix} G_{13}\cos^2\theta + G_{23}\sin^2\theta & (G_{13}-G_{23})\cos\theta\sin\theta \\ (G_{13}-G_{23})\cos\theta\sin\theta & G_{13}\sin^2\theta + G_{23}\cos^2\theta \end{bmatrix} \tag{11}$$

2.3 Governing nonlinear equilibrium equations and solution procedure

The equilibrium equations may be obtained by application of virtual work principle (Chattopadhyay *et al.* 1995) as

$$\{\varphi\} = \oint_A [\bar{B}]^T \{F\} dA - \{P\} = \{0\} \tag{12}$$

where $\{\phi\}$ denotes the resultants of internal and external generalised forces $\{P\}$ and with the help of Eqs. (6), (7) and (8), Eq. (12) becomes

$$\begin{aligned} &\oint_A ([B]+[B'])^T [E]([B]+0.5[B'])dA\{d_e\} - \{P\} = \{0\} \\ &\Rightarrow [K]_s \{d_e\} = \{P\} \end{aligned} \tag{13}$$

where, the secant stiffness matrix $[K]_s$ is given by

$$\begin{aligned} [K]_s = &\oint_A [B]^T [E][B] dA + 0.5\oint_A [B]^T [E][B'] dA \\ &+ \oint_A [B']^T [E][B] dA + 0.5\oint_A [B']^T [E][B'] dA \end{aligned}$$

Taking appropriate variation of Eq. (12) with respect to $\{d_e\}$ the following may be obtained

$$\begin{aligned} d\{\varphi\} &= \oint_A d[\bar{B}]^T \{F\} dA + \oint_A [\bar{B}]^T d\{F\} dA - d\{P\} \\ &= [K]_T \, d\{d_e\} - d\{P\} \end{aligned} \tag{14}$$

Using the relations as given in Eqs. (6), (7) and (8) into Eq. (14), one gets

$$\begin{aligned} &\oint_A d([B]+[B'])^T \{F\} dA \\ &+ \oint_A ([B]+[B'])^T \{E\}([B]+[B'])dA\, d\{d_e\} - d\{P\} = \{0\} \\ &\Rightarrow [K]_F \, d\{d_e\} + ([K]_L + [K]_{LT}) d\{d_e\} = d\{P\} \end{aligned} \tag{15}$$

where

$$[K]_L = \oint_A [B]^T [E][B] dA,$$

$$[K]_F = \oint_A [G']^T \begin{bmatrix} N_x & N_{xy} \\ N_{xy} & N_y \end{bmatrix} [G'] dA,$$

$$[K]_{LT} = \oint_A [B]^T [E][B'] dA + \oint_A [B']^T [E][B] dA + \oint_A [B']^T [E][B'] dA$$

$[K]_F$ is a symmetric matrix dependent on the stress level. This matrix is referred to as the initial stress matrix or the geometric matrix. N_x, N_y and N_{xy} are in-plane force and shear resultants as described Eq. (8). Thus, the tangent stiffness matrix consists of three parts and is expressed as

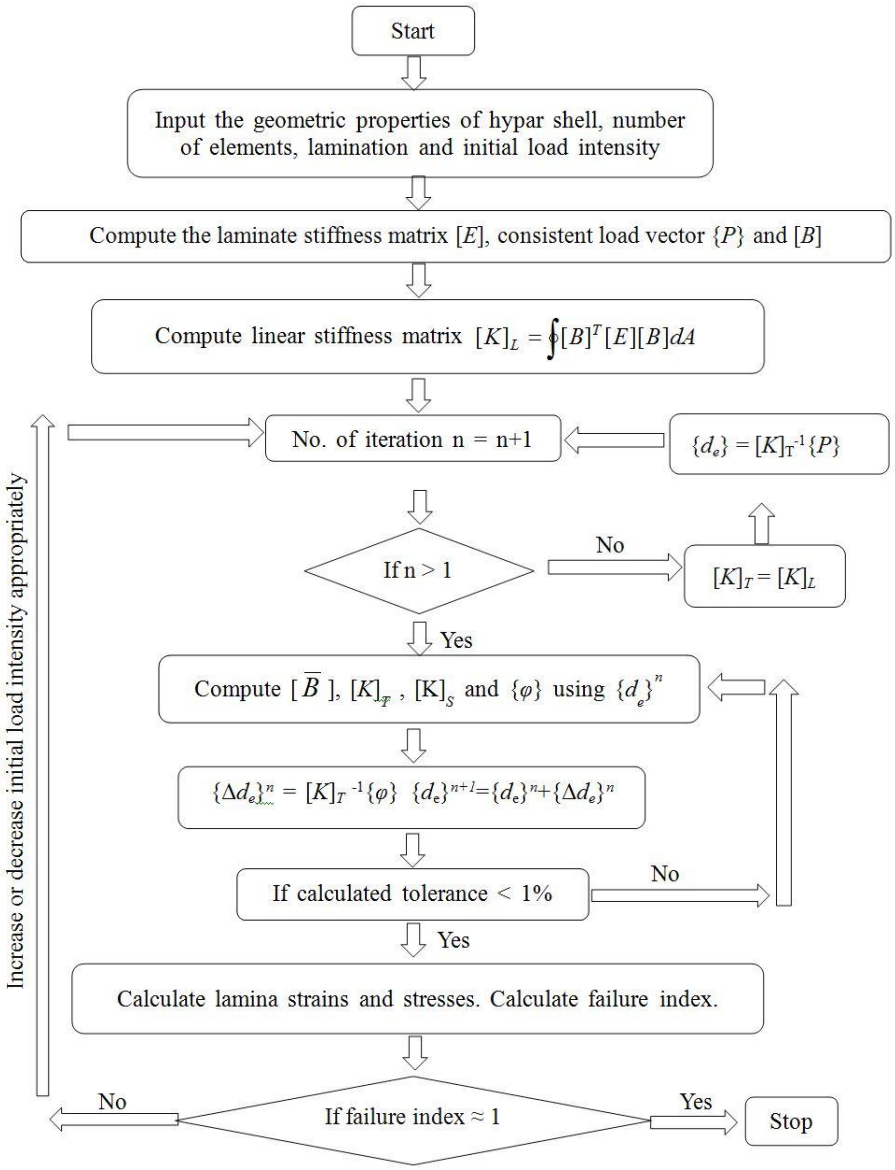

Fig. 2 Algorithm of first ply failure load

$$[K]_T = [K]_L + [K]_{LT} + [K]_F \tag{16}$$

In order to solve nonlinear equilibrium equation Eq. (12) by the Newton-Raphson iteration procedure, the improved solution of $\{d_e\}_{n+1}$ is reached in terms of Taylor's series and the higher order terms are ignored.

$$\{\varphi\}\left(\{d_e\}^{n+1}\right) = \{\varphi\}\left(\{d_e\}^n\right) + \left(\frac{d\{\varphi\}}{d\{d_e\}}\right)_n \{\Delta d_e\}^n = 0 \tag{17}$$

where

$$\{d_e\}^{n+1} = \{d_e\}^n + \{\Delta d_e\}^n \tag{18}$$

In the above equation $\left(\frac{d\{\varphi\}}{d\{d_e\}}\right) = [K]_T$.

Improved values of $\{d_e\}^{n+1}$ are obtained from Eq. (18) by calculating

$$\{\Delta d_e\}^{n+1} = \left([K]_T^n\right)^{-1}\left(\{P\} - [K]_S^n \{d_e\}^n\right) \tag{19}$$

Now, the convergence of this procedure may be checked by using a pre-set tolerance limit (1% is adopted here) which is expressed in Eq. (20). Similar convergence criteria were adopted earlier by Palazotto and Dennis (1992) and Chattopadhyay *et al*. (1995).

$$\sqrt{\left(\{\varphi\}^T\{\varphi\}\right)/\left(\{P\}^T\{P\}\right)} \times 100 \le Tolerance \tag{20}$$

2.4 Lamina stress calculations

Lamina strains are transformed from the global axes of the shell to the local axes of the lamina using transformation matrix (Eq. (21)). Lamina stresses are obtained using the constitutive relations of the lamina (Eq. (22)).

$$\begin{Bmatrix}\varepsilon_1\\ \varepsilon_2\\ \varepsilon_6\end{Bmatrix}=\begin{bmatrix}\sin^2\theta & \cos^2\theta & \sin 2\theta\\ \cos^2\theta & \sin^2\theta & -\sin 2\theta\\ -\sin 2\theta & \sin 2\theta & -2\cos 2\theta\end{bmatrix}\begin{Bmatrix}\varepsilon_x\\ \varepsilon_y\\ \gamma_{xy}\end{Bmatrix} \tag{21}$$

$$\begin{Bmatrix}\sigma_1\\ \sigma_2\\ \sigma_6\end{Bmatrix}=\begin{bmatrix}(1-\nu_{12}\nu_{21})^{-1}E_{11} & (1-\nu_{12}\nu_{21})^{-1}E_{11}\nu_{21} & 0\\ (1-\nu_{12}\nu_{21})^{-1}E_{11}\nu_{21} & (1-\nu_{12}\nu_{21})^{-1}E_{22} & 0\\ 0 & 0 & G_{12}\end{bmatrix}\begin{Bmatrix}\varepsilon_1\\ \varepsilon_2\\ \varepsilon_6\end{Bmatrix} \tag{22}$$

The stress resultants are evaluated at the Gauss points (2 × 2). Lamina stresses and strains are used in well accepted failure theories like maximum stress, maximum strain, Tsai-Hill, Tsai-Wu, Hoffman's, Hashin's and Puck's failure criterion, given below, to evaluate the first ply failure load of the composite skewed hypar shells. The schematic algorithm for computing the first ply failure loads for hypar shells is shown in Fig. 2.

2.5 Maximum stress failure criteria

According to maximum stress theory, the failure initiates if at least one of the criteria is satisfied

$$\begin{aligned}&\text{Fiber breakage mode: } \frac{\sigma_1}{\sigma_{1T}^u}\ge 1,\\ &\text{Fiber buckling mode: } -\sigma_1\ge\sigma_{1C}^u\\ &\text{Matrix cracking mode: } \frac{\sigma_2}{\sigma_{2T}^u}\ge 1,\\ &\text{Matrix crushing mode: } -\sigma_2\ge\sigma_{2C}^u\\ &\text{Matrix shear failure mode: } \frac{\tau_{12}}{\tau_{12}^u}\ge 1\end{aligned} \tag{23}$$

2.6 Maximum strain failure criteria

According to maximum strain theory, the failure initiates if at least one of the criteria is satisfied

$$\begin{aligned}&\text{Fiber breakage mode: } \frac{\varepsilon_1}{\varepsilon_{1T}^u}\ge 1,\\ &\text{Fiber buckling mode: } -\varepsilon_1\ge\varepsilon_{1C}^u\\ &\text{Matrix cracking mode: } \frac{\varepsilon_2}{\varepsilon_{2T}^u}\ge 1,\\ &\text{Matrix crushing mode: } -\varepsilon_2\ge\varepsilon_{2C}^u\\ &\text{Matrix shear failure mode: } \frac{\gamma_{12}}{\gamma_{12}^u}\ge 1\end{aligned} \tag{24}$$

2.7 Tsai-Hill failure criteria

According to Tsai-Hill failure theory, a lamina fails if at least one of the following conditions is satisfied

$$\begin{aligned}&\left(\frac{\sigma_1}{\sigma_{1T}^u}\right)^2+\left(\frac{\sigma_2}{\sigma_{2T}^u}\right)^2-\left(\frac{1}{\sigma_{1T}^u}+\frac{1}{\sigma_{2T}^u}\right)\sigma_1\sigma_2+\left(\frac{\tau_{12}}{\tau_{12}^u}\right)^2\ge 1\\ &\text{for } \sigma_1,\sigma_2>0\\ &\left(\frac{\sigma_1}{\sigma_{1C}^u}\right)^2+\left(\frac{\sigma_2}{\sigma_{2C}^u}\right)^2-\left(\frac{1}{\sigma_{1C}^u}+\frac{1}{\sigma_{2C}^u}\right)\sigma_1\sigma_2+\left(\frac{\tau_{12}}{\tau_{12}^u}\right)^2\ge 1\\ &\text{for } \sigma_1,\sigma_2<0\end{aligned} \tag{25}$$

2.8 Tsai-Wu failure criteria

Tsai-Wu criterion can be expressed as

$$\begin{aligned}&\left(\frac{1}{\sigma_{1T}^u}-\frac{1}{\sigma_{1C}^u}\right)\sigma_1+\left(\frac{1}{\sigma_{2T}^u}-\frac{1}{\sigma_{2C}^u}\right)\sigma_2+\left(\frac{1}{\sigma_{1T}^u\sigma_{1C}^u}\right)\sigma_1^2\\ &+\left(\frac{1}{\sigma_{2T}^u\sigma_{2C}^u}\right)\sigma_2^2-\left(\sqrt{\sigma_{1T}^u\sigma_{1C}^u\sigma_{2T}^u\sigma_{2C}^u}\right)\sigma_1\sigma_2+\left(\frac{\tau_{12}}{\tau_{12}^u}\right)^2\ge 1\end{aligned} \tag{26}$$

2.9 Hoffman's failure criteria

Hoffman's criterion is expressed as

$$\begin{aligned}&\frac{1}{2}\left(\frac{1}{\sigma_{1T}^u\sigma_{1C}^u}-\frac{1}{\sigma_{2T}^u\sigma_{2C}^u}\right)\sigma_1^2+\frac{1}{2}\left(\frac{1}{\sigma_{1T}^u\sigma_{1C}^u}+\frac{1}{\sigma_{2T}^u\sigma_{2C}^u}\right)(\sigma_1-\sigma_2)^2\\ &+\left(\frac{1}{\sigma_{1T}^u}-\frac{1}{\sigma_{1C}^u}\right)\sigma_1+\left(\frac{1}{\sigma_{2T}^u}-\frac{1}{\sigma_{2C}^u}\right)\sigma_2+\left(\frac{\tau_{12}}{\tau_{12}^u}\right)^2\ge 1\end{aligned} \tag{27}$$

2.10 Hashin's failure criteria

$$\begin{aligned}&\text{Fiber breakage mode: } \left(\frac{\sigma_1}{\sigma_{1T}^u}\right)^2+\left(\frac{\tau_{12}}{\tau_{12}^u}\right)^2\ge 1,\\ &\text{Fiber buckling mode: } -\sigma_1\ge\sigma_{1C}^u\\ &\text{Matrix cracking mode: } \left(\frac{\sigma_2}{\sigma_{2T}^u}\right)^2+\left(\frac{\tau_{12}}{\tau_{12}^u}\right)^2\ge 1\\ &\text{Matrix crushing mode: } \left[\left(\frac{\sigma_{2C}^u}{2\tau_{12}^u}\right)^2-1\right]\left(\frac{\sigma_2}{\sigma_{2C}^u}\right)+\left(\frac{\sigma_2}{2\tau_{23}^u}\right)^2+\left(\frac{\tau_{12}}{\tau_{12}^u}\right)^2\ge 1\end{aligned} \tag{28}$$

2.11 Puck's failure criteria

$$\begin{aligned}&\text{Fiber breakage mode: } \frac{1}{2}\left(\left|\frac{\sigma_1}{\sigma_{1T}^u}\right|+\left|\frac{\varepsilon_1}{\varepsilon_{1T}^u}\right|\right)\ge 1,\\ &\text{Fiber buckling mode: } \frac{1}{2}\left(\left|\frac{\sigma_1}{\sigma_{1C}^u}\right|+\left|\frac{\varepsilon_1}{\varepsilon_{1C}^u}\right|\right)\ge 1\\ &\text{Matrix cracking mode A } (\sigma_2>0):\\ &\sqrt{\left(\frac{\tau_{12}}{\tau_{12}^u}\right)^2+\left(1-p_{12}^{(+)}\frac{\sigma_{2T}^u}{\tau_{12}^u}\right)^2\left(\frac{\sigma_2}{\sigma_{2T}^u}\right)^2}+p_{12}^{(+)}\frac{\sigma_2}{\tau_{12}^u}\ge 1\end{aligned}$$

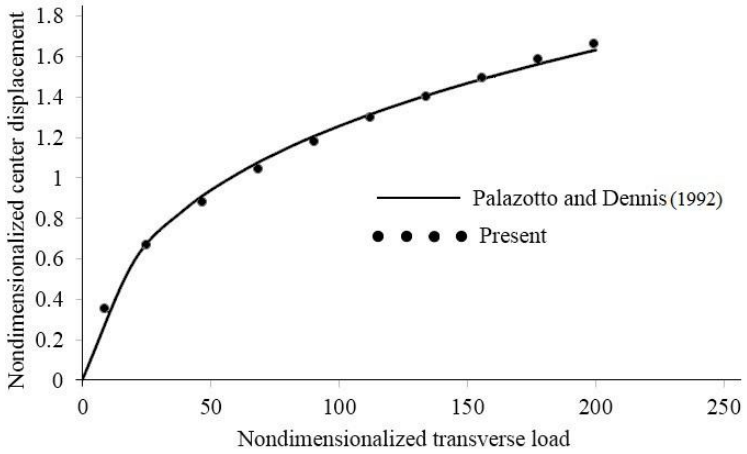

Fig. 3 Nonlinear deflection of isotropic plate

Matrix crushing mode B $\left[(\sigma_2<0);0\le\left|\frac{\sigma_2}{\tau_{12}}\right|\le\frac{\tau_{23}^A}{\left|\tau_{12}^C\right|}\right]$:

$$\frac{1}{\tau_{12}^u}\left[\sqrt{(\tau_{12})^2+\left(p_{12}^{(-)}\sigma_2\right)^2}+p_{12}^{(+)}\sigma_2\right]\ge 1$$

Matrix crushing mode C $\left[(\sigma_2<0);0\le\left|\frac{\tau_{12}}{\sigma_2}\right|\le\frac{\left|\tau_{12}^C\right|}{\tau_{23}^A}\right]$:

$$\left[\left\{\frac{\tau_{12}}{2\left(1+p_{12}^{(-)}\tau_{23}^A\right)}\right\}^2+\left(\frac{\sigma_2}{\sigma_{2C}^u}\right)^2\right]\frac{\sigma_{2C}^u}{(-\sigma_2)}\ge 1$$

where

$$p_{12}^{(+)}=0.3,\quad p_{12}^{(-)}=0.3,$$

$$\tau_{23}^A=\frac{\tau_{12}^u}{2p_{12}^{(-)}}\left[\sqrt{1+2p_{12}^{(-)}\frac{\sigma_{2C}^u}{\tau_{12}^u}}-1\right] \qquad (29)$$

and $$\tau_{12}^C=\tau_{12}^u\sqrt{1+2p_{12}^{(-)}\frac{\tau_{23}^A}{\tau_{12}^u}}$$

In case of interactive failure theories such as Tsai-Hill, Tsai-Wu and Hoffman's failures criteria, none of the individual lamina stress components reach the permissible values but their interaction leads to failure. In case of such failures, the individual stress values developed may be compared to their corresponding permissible values to investigate that which stress component contributing to a particular interactive criterion plays the most significant role in the failure. The stress component for which the ratio of the developed to permissible stress is nearest to unity may be identified as the most significant component contributing to the failure following the corresponding failure mode also.

2.12 Step by step solution procedure of first ply failure analysis

Step 1: The static displacement fields of shells are calculated for the external load $\{P\}$. To obtain the linear first ply failure load values the linear displacement fields are used while the converged nonlinear displacement fields are used for getting the nonlinear failure load values.

Step 2: The strain vectors considering the linear and nonlinear terms are calculated at four Gauss points from the linear and nonlinear displacement fields and these strains are combined to obtain the mid-surface strain vector following Eq. (6).

Step 3: The in-plane and transverse strains are transformed from global to local axes system using Eq. (21).

Step 4: Using Eq. (22) the lamina stresses are calculated at Gauss points. Linear strains are used to compute the linear failure load values. The nonlinear failure load values are calculated using the nonlinear strain terms.

Step 5: The stresses are extrapolated from Gauss point locations to the element node points.

Step 6: The lamina stresses are incorporated in the different failure theories and the failure index is calculated (refer Reddy and Reddy 1992).

Step 7: The initial external load is appropriately increased or decreased depending on whether the failure index value is lesser than or greater than unity respectively.

Step 8: Steps 1 to 7 are repeated till the percentage difference between the first ply failure load values obtained from two successive iterations is less than unity.

3. Numerical examples

In order to validate the geometrically nonlinear finite element formulation the authors compare the nondimensional static central deflection values, considering geometric nonlinear strains of simply supported isotropic plates, obtained by Palazotto and Dennis (1992) with the values obtained from present formulation. The comparison of these results is shown in Fig. 3. The uniformly distributed transverse load and central deflection are nondimensionalized as $\bar{q} = (q_0a^4)/(E_{11}h^4)$ and $\bar{w} = w/h$ respectively.

The nonlinear first ply failure load values of laminated composite plate with partially clamped edge condition

Table 1 Comparison of first ply failure loads in Newton for a $(0_2^0/90^0)_2$ plate

Failure criteria	Length/ plate thickness	Experimental failure load (Kam *et al*. 1996)	First ply failure loads (Kam *et al*. 1996)	First ply failure loads (present formulation)
Maximum stress	105.26	157.34	147.61	139.94
Maximum strain			185.31	194.58
Hoffman's			143.15	137.12
Tsai-Wu			157.78	150.71
Tsai-Hill			144.42	151.22

* Length = 100 mm; load details = central point load

Table 2 Nondimensional natural frequencies for (θ / –θ / θ) graphite-epoxy twisted plates

Angle of twist	θ (degree)	0	15	30	45	60	75	90
ϕ = 15°	Qatu and Lessia (1991)	1.0035	0.9296	0.7465	0.5286	0.3545	0.2723	0.2555
	Present formulation	0.9985	0.9250	0.7444	0.5280	0.3542	0.2720	0.2552
ϕ = 30°	Qatu and Lessia (1991)	0.9566	0.8914	0.7205	0.5149	0.3443	0.2606	0.2436
	Present formulation	0.9501	0.8841	0.7180	0.5143	0.3446	0.2611	0.2446

* E_{11} = 138 GPa; E_{22} = 8.96 GPa, G_{12} = 7.1 GPa; v_{12} = 0.3; a/b = 1; a/h = 100

Table 3 Material properties of Q–1115 graphite-epoxy

Material constants values	E_{11} 142.5 GPa	$E_{22} = E_{33}$ 9.79 GPa	$G_{12} = G_{13}$ 4.72 GPa	G_{23} 1.192 GPa	$v_{12} = v_{23}$ 0.27	v_{13} 0.25
Strengths values	σ_{1T}^u 2193.5 MPa	σ_{1C}^u 2457 MPa	σ_{2T}^u 41.3 MPa	σ_{2C}^u 206.8 MPa	τ_{13}^u 61.28 MPa	$\tau_{12}^u = \tau_{23}^u$ 78.78 MPa
	ε_{1T}^u 0.01539	ε_{1C}^u 0.01724	ε_{2T}^u 0.00412	ε_{2C}^u 0.02112	γ_{13}^u 0.05141	$\gamma_{12}^u = \gamma_{23}^u$ 0.01669

reported by Kam *et al*. (1996) are compared with those obtained from present formulation in Table 1. The composite plate is subjected to a central point load.

Table 2 furnishes the nondimensional fundamental frequency values of composite twisted plates. Different angle of twists and stacking orders were considered to calculate the frequency values by Qatu and Leissa (1991)) which are compared with the values obtained by the present code. This validation problem is chosen to ensure the proper incorporation of the skewed hypar shell geometry in the present code. This validation problem is chosen to ensure the proper incorporation of the skewed hypar shell geometry in the present computer code.

Apart from benchmark problems, a number of numerical experiments are carried out for different graphite-epoxy [material properties are shown in Table 3 (refer Kam *et al*.

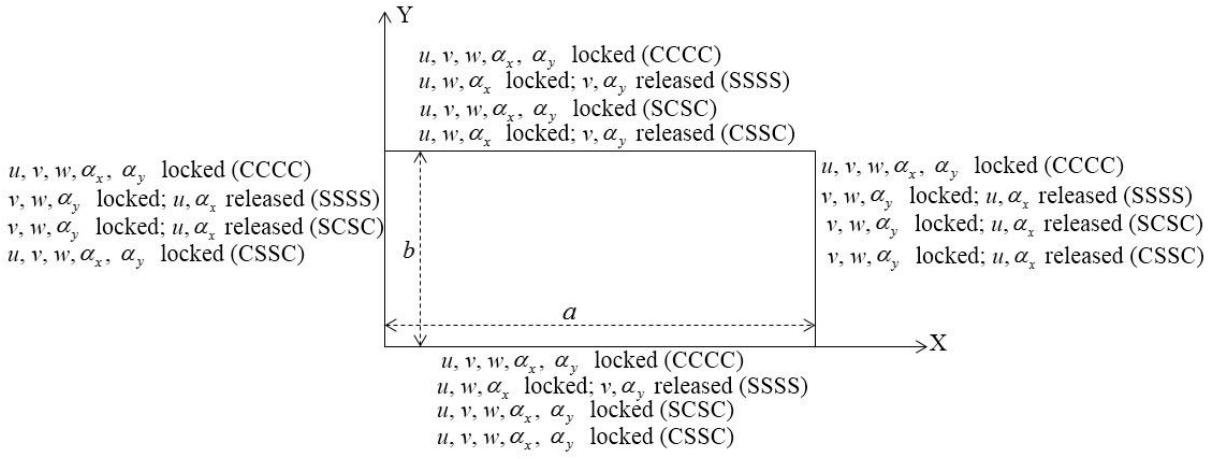

Fig. 4 Schematic representation of all boundary conditions

Table 4 Nondimensionalized nonlinear collapse failure loads $\overline{FL}$ for SSSS

Laminations	Failure criteria	$\overline{FL}$	Failure zone	Failed ply	Failure mode / failure tendency
ASCP	Maximum stress	7990.81	A	1	Matrix shear failure
	Maximum strain	7990.81	A	1	Matrix shear failure
	Hoffman's	*7540.35*	*A*	*1*	*Matrix shear failure*
	Tsai-Hill	7941.78	A	1	Matrix shear failure
	Tsai-Wu	7557.71	A	1	Matrix shear failure
	Hashin's	7932.58	A	1	Matrix cracking
	Puck's	7804.90	A	1	Matrix cracking mode A
	Serviceability	2642.49	A	…	…
SYCP	Maximum stress	7431.05	A	1	Matrix shear failure
	Maximum strain	7431.05	A	1	Matrix shear failure
	Hoffman's	*6842.70*	*A*	*2*	*Matrix shear failure*
	Tsai-Hill	7386.11	A	1	Matrix shear failure
	Tsai-Wu	6846.78	A	2	Matrix shear failure
	Hashin's	7379.98	A	1	Matrix cracking
	Puck's	7263.53	A	1	Matrix cracking mode A
	Serviceability	2636.36	D	…	…
ASAP	Maximum stress	8372.83	A	1	Matrix cracking
	Maximum strain	*6309.50*	*A*	*1*	*Matrix cracking*
	Hoffman's	8229.83	A	1	Matrix cracking
	Tsai-Hill	8921.35	A	1	Matrix cracking
	Tsai-Wu	7515.83	A	1	Matrix cracking
	Hashin's	8357.51	A	1	Matrix cracking
	Puck's	8355.46	A	1	Matrix cracking mode A
	Serviceability	9751.79	D	…	…
SYAP	Maximum stress	12233.91	A	1	Matrix cracking
	Maximum strain	*10103.17*	*A*	*1*	*Matrix cracking*
	Hoffman's	12052.09	A	1	Matrix cracking
	Tsai-Hill	13162.41	A	1	Matrix cracking
	Tsai-Wu	11398.36	A	1	Matrix cracking
	Hashin's	12213.48	A	1	Matrix cracking
	Puck's	12210.42	A	1	Matrix cracking mode A
	Serviceability	16377.94	C	…	…

* $a/b = 1$; $a/h = 100$; $c/a = 0.2$

1996)] skewed hypar shell options obtained by combining different boundary conditions of clamped (C) and simply supported (S) edges and laminations under uniformly distributed load. The present study considers the shallow hypar shell options only (height to shorter span ratio is equal to 0.2) as, from practical engineering point of view, shells with deep curvatures are difficult to cast and fabricate. The failure loads are obtained for two regular (SSSS and CCCC) and two irregular (SCSC and CSSC) boundary conditions which are described in Fig. 4. For each boundary condition, two and three layered anti-symmetric (AS) and symmetric (SY), cross (CP) and angle ply (AP) laminations are taken up. The $0^0/90^0$ (ASCP), $0^0/90^0/0^0$ (SYCP) cross ply laminates and 45^0/-45^0 (ASAP), 45^0/-$45^0/45^0$ (SYAP) angle ply laminates are considered here to obtain the first ply failure load values (FL) which are nondimensionalized as $\overline{FL} = (FL/E_{22})(a/h)^4$. The plies are numbered from top to bottom of the laminate. Other related information are furnished in Tables 4 to 7. According to the above mode of designating the shell options, a SCSC/SYAP symbol means a symmetric angle ply shell simply supported along $x = 0$, clamped along $y =$ b, simply supported along $x = a$ and clamped along $y = 0$ taken in order.

Table 5 Nondimensionalized nonlinear collapse failure loads $\overline{FL}$ for CCCC

Laminations	Failure criteria	$\overline{FL}$	Failure zone	Failed ply	Failure mode / failure tendency
ASCP	Maximum stress	11908.07	C	2	Matrix shear failure
	Maximum strain	11908.07	C	2	Matrix shear failure
	Hoffman's	10879.47	A	1	Matrix shear failure
	Tsai-Hill	11646.58	D	2	Matrix shear failure
	Tsai-Wu	11066.39	C	2	Matrix shear failure
	Hashin's	11638.41	C	2	Matrix cracking
	Puck's	*4775.28*	*A*	*2*	*Matrix crushing mode C*
	Serviceability	3883.55	B	…	…
SYCP	Maximum stress	10972.42	A	1	Matrix cracking
	Maximum strain	10836.57	A	1	Matrix cracking
	Hoffman's	10781.41	A	1	Matrix cracking
	Tsai-Hill	10890.70	A	1	Matrix cracking
	Tsai-Wu	10812.05	A	1	Matrix cracking
	Hashin's	10839.63	A	1	Matrix cracking
	Puck's	*3485.19*	*A*	*1*	*Matrix crushing mode C*
	Serviceability	3656.79	B	…	…
ASAP	Maximum stress	10755.87	A	1	Matrix cracking
	Maximum strain	*9463.74*	*A*	*1*	*Matrix cracking*
	Hoffman's	10692.54	A	1	Matrix cracking
	Tsai-Hill	11251.28	A	1	Matrix cracking
	Tsai-Wu	10315.63	A	1	Matrix cracking
	Hashin's	10726.25	A	1	Matrix cracking
	Puck's	10721.14	A	1	Matrix cracking mode A
	Serviceability	20007.15	B	…	…
SYAP	Maximum stress	14263.53	A	1	Matrix cracking
	Maximum strain	*13082.74*	*A*	*1*	*Matrix cracking*
	Hoffman's	14184.88	A	1	Matrix cracking
	Tsai-Hill	14626.15	A	1	Matrix cracking
	Tsai-Wu	13875.38	A	1	Matrix cracking
	Hashin's	14203.27	A	1	Matrix cracking
	Puck's	14192.03	A	1	Matrix cracking mode A
	Serviceability	19281.92	B	…	…

* $a/b = 1$; $a/h = 100$; $c/a = 0.2$

Table 6 Nondimensionalized nonlinear collapse failure loads $\overline{FL}$ for SCSC

Laminations	Failure criteria	$\overline{FL}$	Failure zone	Failed ply	Failure mode / failure tendency
ASCP	Maximum stress	11030.64	A	1	Matrix shear failure
	Maximum strain	11030.64	A	1	Matrix shear failure
	Hoffman's	10140.96	A	1	Matrix shear failure
	Tsai-Hill	10928.50	A	1	Matrix shear failure
	Tsai-Wu	*10131.77*	*A*	*1*	*Matrix shear failure*
	Hashin's	10897.85	A	1	Matrix cracking
	Puck's	10667.01	A	1	Matrix cracking mode A
	Serviceability	2594.48	B	…	…

* $a/b = 1$; $a/h = 100$; $c/a = 0.2$

Table 6 Continued

Laminations	Failure criteria	$\overline{FL}$	Failure zone	Failed ply	Failure mode / failure tendency
SYCP	Maximum stress	10127.68	A	1	Matrix cracking
	Maximum strain	10197.14	A	1	Matrix cracking
	Hoffman's	*8131.77*	*A*	*1*	*Matrix shear failure*
	Tsai-Hill	8813.07	A	1	Matrix shear failure
	Tsai-Wu	8171.60	A	1	Matrix shear failure
	Hashin's	8729.31	A	1	Matrix cracking
	Puck's	8524.00	A	1	Matrix cracking mode A
	Serviceability	2497.45	B	…	…
ASAP	Maximum stress	10398.36	A	1	Matrix cracking
	Maximum strain	*8805.92*	*A*	*1*	*Matrix cracking*
	Hoffman's	10293.16	A	1	Matrix cracking
	Tsai-Hill	11069.46	A	1	Matrix cracking
	Tsai-Wu	9808.99	A	1	Matrix cracking
	Hashin's	10382.02	A	1	Matrix cracking
	Puck's	10377.94	A	1	Matrix cracking mode A
	Serviceability	13488.25	A	…	…
SYAP	Maximum stress	14042.90	A	1	Matrix cracking
	Maximum strain	*11676.20*	*A*	*1*	*Matrix cracking*
	Hoffman's	13900.92	A	1	Matrix cracking
	Tsai-Hill	14909.09	A	1	Matrix cracking
	Tsai-Wu	13230.85	A	1	Matrix cracking
	Hashin's	14010.21	A	1	Matrix cracking
	Puck's	14005.11	A	1	Matrix cracking mode A
	Serviceability	14834.52	B	…	…

* $a/b = 1$; $a/h = 100$; $c/a = 0.2$

4. Results and discussions

The results of the numerical experiments are discussed in this section considering the benchmark problems and the additional examples taken up by the authors.

4.1 Benchmark problems

The close agreement of present and published nondimensionalized deflection results shown in Fig. 3 indicates the correct incorporation of the geometrically nonlinear strain terms in bending formulation of the present finite element code. The first ply failure load values obtained from different failure criteria of a composite plate are compared with those obtained from the present formulation in Table 1 and this comparison proves the accuracy of the first ply failure formulation through finite element. In these two benchmark problems the authors convert the skewed hypar shell geometry to a plate configuration by assigning a very high value of radius of cross curvature ($R_{xy} = 10^{30}$). The nondimensionalized fundamental frequencies of twisted plates which are structurally similar to skewed hypar shell geometries are furnished in Table 2 and the present results show extremely good agreement with the published ones. This establishes the fact that the skewed hypar shell geometry is properly modelled in the present finite element code. The authors use a simple lumped mass matrix scheme along with the undamaged stiffness matrix to solve the frequency values.

4.2 Behaviour of cross and angle ply hypar shells of different boundary conditions from collapse criteria

The minimum value of the failure load obtained from different failure criteria (Eqs. (23) to (29)) is considered as the acceptable failure load on which the engineering factor of safety should be imposed to get the working load values. These collapse failure loads are shown in italics in the corresponding Tables 4 to 7.

The nondimensionalized nonlinear first ply failure load values are reported for two regular boundary conditions (SSSS and CCCC) in Tables 4 and 5 respectively. For both these two boundary conditions, anti-symmetric laminates perform better than symmetric ones in terms of first ply failure loads for cross ply shells but among the angle ply shells the reverse trend is observed. Again, on comparing cross and angle ply laminates mutually it is found that the

Table 7 Nondimensionalized nonlinear collapse failure loads $\overline{FL}$ for CSSC

Laminations	Failure criteria	$\overline{FL}$	Failure zone	Failed ply	Failure mode / failure tendency
ASCP	Maximum stress	10520.94	B	2	Matrix shear failure
	Maximum strain	10520.94	B	2	Matrix shear failure
	Hoffman's	8364.66	A	1	Matrix shear failure
	Tsai-Hill	10477.02	B	2	Matrix shear failure
	Tsai-Wu	9004.08	A	1	Matrix shear failure
	Hashin's	10329.93	B	1	Matrix crushing
	Puck's	*3677.22*	*A*	*2*	*Matrix crushing mode C*
	Serviceability	3313.58	B	…	…
SYCP	Maximum stress	9850.87	A	1	Matrix cracking
	Maximum strain	9871.30	A	1	Matrix cracking
	Hoffman's	8566.90	A	1	Matrix cracking
	Tsai-Hill	9073.54	A	1	Matrix cracking
	Tsai-Wu	8611.85	A	1	Matrix cracking
	Hashin's	8991.83	A	1	Matrix cracking
	Puck's	*3094.99*	*A*	*2*	*Matrix crushing mode C*
	Serviceability	3074.56	B	…	…
ASAP	Maximum stress	10355.46	A	1	Matrix cracking
	Maximum strain	*7564.86*	*A*	*1*	*Matrix cracking*
	Hoffman's	9745.66	A	1	Matrix cracking
	Tsai-Hill	11432.07	A	1	Matrix cracking
	Tsai-Wu	8938.71	A	1	Matrix cracking
	Hashin's	10354.44	A	1	Matrix cracking
	Puck's	10354.44	A	1	Matrix cracking mode A
	Serviceability	12265.58	C	…	…
SYAP	Maximum stress	13252.30	A	1	Matrix cracking
	Maximum strain	*10970.38*	*A*	*1*	*Matrix cracking*
	Hoffman's	13078.65	A	1	Matrix cracking
	Tsai-Hill	13833.50	A	1	Matrix cracking
	Tsai-Wu	12371.81	A	1	Matrix cracking
	Hashin's	13216.55	A	1	Matrix cracking
	Puck's	13209.40	A	1	Matrix cracking mode A
	Serviceability	16442.29	B	…	…

* $a/b = 1$; $a/h = 100$; $c/a = 0.2$

failure load values of SYAP laminates are 1.3 and 2.7 times of the failure load values of ASCP laminates for SSSS and CCCC boundary conditions respectively. Thus, SYAP laminate i.e., $45^0/-45^0/45^0$ turns out to be the best shell option among all the shell combinations considered here for SSSS and CCCC.

The close look at the results furnished in Tables 6 and 7 for two irregular boundary conditions (SCSC and CSSC) reflect that, like regular boundary conditions, the first ply failure load values of symmetric angle ply laminates are higher than those of anti-symmetric angle ply laminates. For the cases of cross ply shells, anti-symmetric laminates are good compared to the symmetric ones. The load bearing capacities of SYAP shells are approximately 1.15 and 2.98 times of that of ASCP shells respectively. So it can safely be concluded that among all the cases considered here, the SYAP shells ($45^0/-45^0/45^0$) are the best choices to the practicing design engineers.

For all the angle ply shells, the maximum strain criterion gives the minimum collapse failure load values for all four different boundary conditions taken up here. The Puck's criterion is the governing criteria for cross ply shells for CSSC and CCCC boundary conditions respectively. For SSSS and SCSC cross ply shells the Hoffman's failure criterion governs the failure loads in all of the cases except one. In this exceptional case (SCSC/ASCP) also, though the Tsai-Wu criterion yields the minimum failure load but such value is very close to that obtained through Hoffman's

criterion. Interestingly, for SSSS and SCSC cross ply shells the failure loads obtained through Puck's criterion are not by far out (within 6%) when compared to the Hoffman's failure load. Thus it would not be incorrect from engineering standpoint to state that Puck's criterion may only be used to evaluate first ply failure loads of cross ply shells for all the four boundary conditions taken up here.

It is observed from the results furnished in Tables 4 to 7 that the differences between the first ply failure load values obtaining from different failure criteria are large. This phenomenological wide variation is due to the difference in the basic formulation of these criteria. Hence it is difficult to find any physical reasons for this. These similar type of observations were also noticed in the research works of some earlier researchers like Soni (1983) and Reddy and Reddy (1992).

4.3 Behaviour of shells with different boundary conditions from serviceability standpoint

Besides the collapse criteria, the present authors consider the failure load from serviceability point of view with the permissible deflection of the skewed hypar shell taken as shorter span/250. The results reported in Tables 4 to 7 establish the fact that the first ply failure loads from serviceability point of view are highest when all the edges are clamped (CCCC) and lowest for SCSC shells except for anti-symmetric angle ply shell. For this exceptional case, SSSS edge condition gives the minimum failure load from serviceability criterion.

It is also interesting to note that for most of the cross ply laminates, the first ply failure loads obtained through collapse criteria yield higher values compared to those obtained from serviceability consideration and for all angle ply laminates, the failure load values obtained from serviceability consideration yield higher values compared to those obtained from collapse criteria. Hence, the cross ply laminates behave like ductile materials and there is an apprehension of brittle failure for angle ply class of shells. This is very helpful information to the practicing designers designing civil engineering composite shell roofs in earthquake prone zones.

4.4 Effect of boundary condition on first ply failure loads obtained from collapse criteria

The results furnished in Tables 4 to 7 show that the SCSC boundary condition gives the highest magnitude of first ply failure collapse load values and CSSC condition gives the lowest values of first ply failure loads for all cross ply shells. The CCCC and SSSS boundary conditions give the maximum and minimum first ply failure loads from collapse consideration for all angle ply shells respectively. The failures of the angle ply shells are through the matrix cracking mode because for all angle ply laminates, the fibers run along diagonal directions and the matrix is reinforced enough by the fibers to prevent its failure through matrix shear failure mode or matrix crushing mode C in contrast to failure of cross ply laminates. It is interestingly noticed for cross ply shells, that the failure load values decrease noticeably for two adjacent edges clamped (CSSC) and for all four edges clamped (CCCC) shells when compared with those values obtained for SSSS and SCSC shells. This behaviour may be explained as given below. A skewed hypar shell has an anticlastic geometry with a sagging curvature along one of its diagonals and a hogging curvature along the other diagonal. By virtue of the geometry of the skewed hypar shell the forces and moments are transformed through its diagonal directions and when two adjacent edges are clamped as in CSSC and CCCC cases, the loads tend to get transferred in the diagonal directions. But due to insufficient fibers in matrix along this load transfer path, the matrix is weak and the cross ply laminates fail through matrix crushing mode C at a comparatively lower failure load. On the other hand, two adjacent edges are not clamped in SCSC and SSSS shells and the influence of edge conditions on failure loads and failure modes which are discussed above are not applicable.

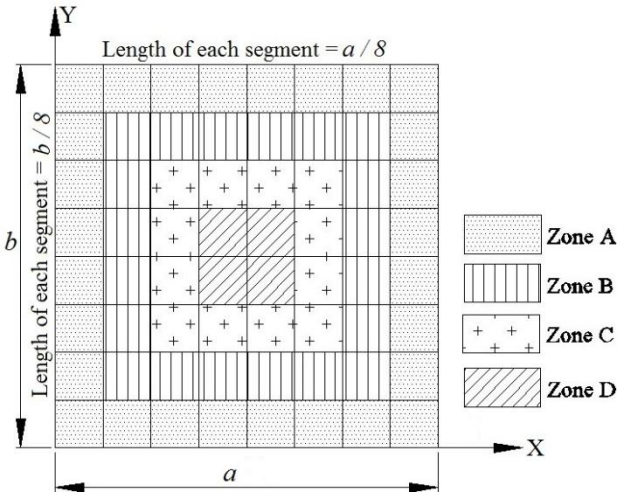

Fig. 5 Failure zones of a hypar shell in plan

The behaviour reported above establishes a close interaction between boundary conditions and laminations which decides finally the failure load value that a particular shell combination can withstand. In fact the isotropic shells behave in a completely different way and highest failure load is achieved when all the four edges are clamped.

4.5 Failure zones of hypar shells and guidelines for non-destructive test monitoring

The authors classify the hypar shell geometry into four different zones in plan. These zones are classified as Zones A, B, C and D and shown in Fig. 5. The location of the first ply failure point is extremely important to be known to a practicing engineer because any instrumentation needed for hidden flaw detection should start from that point. Zone A is the most vulnerable zone of all the cross and angle ply shells considered here as failure initiates from this zone as evident from the results shown in Tables 4 to 7. This indicates that any instrumentation for non-destructive health assessment may be restricted within this peripheral zone only.

Apart from preventing a material failure the maximum value of deflection should be limited to an upper value of

shorter span / 250 to meet the serviceability requirements. Tables 4 to 7 indicate the zones which are prone to undergo maximum deflection for different boundary conditions and laminations. Periodic monitoring of deflections of these zones is also important if a shell has any chance of getting overloaded.

4.6 Suggesting partial factor of safety values on first ply failure loads

The design codes outline methods of evaluating working load values which can be safely put on a structural surface satisfying parallely the conditions of collapse and serviceability. In the present study the load corresponding to a maximum deflection of shorter span / 250 is taken as the working load. Naturally, when the first ply failure load values are greater than the working loads, factor of safety values may be suggested as ratios of the first ply failure loads to the working loads. These values are furnished in Table 8 rounded up to the nearest quarter of an integer. In some cases, for angle ply shells, the maximum deflection limit is reached after initiation of material failure. In these cases the first ply failure loads itself may be taken as the working loads and hence the corresponding factor of safety is suggested to be unity.

Table 8 Proposed partial factors of safety for load

Lamination	Boundary conditions			
	SSSS	SCSC	CSSC	CCCC
ASCP	Proposed partial factors of safety			
	3	4	1.25	1.25
SYCP	2.75	3.5	1.25	1
ASAP	1	1	1	1
SYAP	1	1	1	1

4.7 Relative performances of different shell options and selection guidelines

For a given quantity of material consumption an engineer has different options to choose combining angle and cross ply laminates of anti-symmetric and symmetric stacking orders. Thus one should seek an optimal selection keeping in mind the practical requirements. An engineer may restrained the edges differently to simulate a simply supported or a clamped boundary condition. When the performances of different shell options are carefully observed it is found that though specific trends are there from some angle but the exceptions cannot be ignored fully. This is why in Table 9 ranks are assigned to the different shell options from collapse and serviceability performance points of view. To get an overall picture combining the two performance criteria the summation of ranks are also furnished.

The relative superior performance of angle ply laminates compared to cross ply ones is well-established through the present study. Out of the sixteen shell combinations taken up here only angle ply shells come within the first eight in terms of deflection but when the shells are ranked in terms of material failure two of the cross ply combinations (SCSC/ASCP and SCSC/SYCP) figure within the first eight ranks. When the sum of the ranks are considered it is found that the angle ply combinations are by and large much better than the cross ply ones except the fact that the SCSC/ASCP shell is better than the SSSS/ASAP shell. This

Table 9 Ranks of shell combinations from different performance criteria

Shell options	Rank in terms of		Sum of ranks
	Collapse load from failure criteria	Load corresponding to serviceability failure	
SSSS/ASCP	10	13	23
SSSS/SYCP	11	14	25
SSSS/ASAP	12	8	20
SSSS/SYAP	5	4	9
SCSC/ASCP	4	15	19
SCSC/SYCP	8	16	24
SCSC/ASAP	7	6	13
SCSC/SYAP	2	5	7
CSSC/ASCP	14	11	25
CSSC/SYCP	16	12	28
CSSC/ASAP	9	7	16
CSSC/SYAP	3	3	6
CCCC/ASCP	13	9	22
CCCC/SYCP	15	10	25
CCCC/ASAP	6	1	7
CCCC/SYAP	1	2	3

	Shell options	Rank in terms of		Sum of ranks
		Collapse load from failure criteria	Load corresponding to serviceability failure	
Boundary condition	CCCC	35	22	57
	CSSC	42	33	75
	SCSC	21	42	63
	SSSS	38	39	77
Lamination	AP	45	36	81
	CP	91	100	191
	SY	61	66	127
	AS	75	70	145

indicates that, with suitable adjustment of boundary conditions and lamina stacking order a cross ply shell may also show a good performance.

When overall performances of the different boundary conditions are only focussed on, the CCCC edge condition proves to be the best. Interestingly, so far tendency of material failure is concerned the above boundary condition is not the best option, SCSC shells perform even better.

When angle and cross ply laminates are compared the former shows overall better performances and also in individual material failure and serviceability criteria. Similarly symmetric laminates are convincingly better in performance when compared with the anti-symmetric ones.

5. Conclusions

The following conclusions are drawn from the present study.

- The finite element formulation, which is used for the present study, accurately models the geometrically nonlinear first ply failure behavior of laminated composite hypar shell roofs as the results of the benchmark problems show extremely good agreement with the published ones.
- The failure load values of the composite hypar shells for different edge conditions are presented systematically which are expected to serve as valuable design aids to practicing engineers.
- Generally the angle ply laminates perform better than the cross ply ones in terms of their first ply failure load values. The SYAP shell (45^0/-45^0/45^0) is the best options among all the boundary conditions taken up here.
- Comparing the failure loads obtained from collapse and serviceability criteria, it may be concluded that the cross ply laminates behave like ductile materials but the angle ply shells show tendencies of brittle failure.
- The present study establishes a close interaction between boundary condition and stacking sequence to determine the value of the first ply failure load.
- The probable failure zones for the different shell combinations which are indicated in this paper will be useful for engineers engaged in nondestructive health monitoring of these structural units.
- The practicing engineer may readily refer to the factor of safety values indicated in this paper to assess the safe values of the loads which the shell units can withstand.
- The different shell combinations are assigned ranks against their relative performances both in terms of failure loads and deflections. These ranks are expected to form a useful basis for selection of a particular shell combination in place of another.

References

Adali, S. and Cagdas, I.U. (2011), "Failure analysis of curved composite panels based on first-ply and buckling failures", *Proc. Eng.*, **10**, 1591-1596. https://doi.org/10.1016/j.proeng.2011.04.266

Arciniega, R.A. and Reddy, J.N. (2007), "Tensor-based finite element formulation for geometrically nonlinear analysis of shell structures", *Comp. Meth. App. Mech. Engg.*, **196**, 1048-1073. https://doi.org/10.1016/j.cma.2006.08.014

Bakshi, K. and Chakravorty, D. (2013), "Relative static and dynamic performances of composite conoidal shell roofs", *Steel Comp. Struct., Int. J.*, **15** (4), 379-397. https://doi.org/10.12989/scs.2013.15.4.379

Bakshi, K. and Chakravorty, D. (2014), "Geometrically linear and nonlinear first ply failure loads of composite cylindrical shells", *J. Eng. Mech.-ASCE*, **140**(12). https://doi.org/10.1061/(ASCE)EM.1943-7889.0000808

Bandyopadhyay, T. and Karmakar, A. (2015), "Bending characteristics of delaminated cross-ply composite shallow conical shells in hygrothermal environment", *J. Reinf. Plast. Compos.*, **34**(20), 1724-1735. https://doi.org/10.1177/0731684415596379

Chang, R.R. and Chiang, T.H. (2010), "Theoretical and experimental predictions of first ply failure of a laminated composite elevated floor plate", *Proc. Inst. Mech. Eng. Part E: J. Pro. Mech. Eng.*, **224**(4), 233-245. https://doi.org/10.1243/09544089JPME327

Chattopadhyay, B., Sinha, P.K. and Mukhopadhyay, M. (1995) "Geometrically nonlinear analysis of composite stiffened plates using finite elements", *Compos. Struct.*, **31**, 107-118. https://doi.org/10.1016/0263-8223(95)00004-6

Chen, J.F., Morozov, E.V. and Shankar, K. (2012), "A combined elastoplastic damage model for progressive failure analysis of composite materials and structures", *Compos. Struct.*, **94**(12), 3478-3489. https://doi.org/10.1016/j.compstruct.2012.04.021

Chen, J.F., Morozov, E.V. and Shankar, K. (2014), "Simulating progressive failure of composite laminates including in-ply and delamination damage effects", *Compos.-Part A*, **61**, 185-200. https://doi.org/10.1016/j.compositesa.2014.02.013

Chróścielewski J., Sabik, A., Sobczyk, B. and Witkowski, W. (2016), "Nonlinear FEM 2D failure onset prediction of composite shells based on 6-parameter shell theory", Thin-Walled Struct., **105**, 207-219. https://doi.org/10.1016/j.tws.2016.03.024

Coelho, A.M.G., Mottram, J.T. and Harries, K.A. (2015), "Finite element guidelines for simulation of fibre-tension dominated failures in composite materials validated by case studies", *Compos. Struct.*, **126**, 299-313. https://doi.org/10.1016/j.compstruct.2015.02.071

Das, H.S. and Chakravorty, D. (2007), "Design aids and selection guidelines for composite conoidal shell roofs-a finite element application", *J. Reinf. Plast. Compos.*, **26**(17), 1793-1819. https://doi.org/10.1177/0731684407081380

Dey, S. and Karmakar, A. (2012), "Dynamic analysis of delaminated composite conical shells under low velocity impact", *J. Reinf. Plast. Compos.*, **32**(6), 380-392. https://doi.org/10.1177/0731684412465663

Dong, H., Wanga, J. and Karihaloo, B.L. (2014), "An improved Puck's failure theory for fibre reinforced composite laminates including the in situ strength effect", *Compos. Sci. Tech.*, **98**, 86-92. https://doi.org/10.1016/j.compscitech.2014.04.009

Ellul, B., Camilleri, D. and Betts, C. (2014), "A progressive failure analysis applied to fiber reinforced composite plates subject to out-of- plane bending", *J. Mech. Compos. Mat.*, **49**(6), 605-620. https://doi.org/10.1007/s11029-013-9377-8

Gadade, A.M., Lal, A. and Singh, B.N. (2016a), "Accurate stochastic initial and final failure of laminated plates subjected to hygro-thermo-mechanical loadings using Puck's failure criteria", *Int. J. Mech. Sci.*, **114**, 177-206. https://doi.org/10.1016/j.ijmecsci.2016.05.015

Gadade, A.M., Lal, A. and Singh, B.N. (2016b), "Finite element implementation of Puck's failure criterion for failure analysis of laminated plate subjected to biaxial loadings", *Aeros. Sci. Tech.*, **55**, 227-241. https://doi.org/10.1016/j.ast.2016.05.001

Ganesan, R. and Liu, D.Y. (2008), "Progressive failure and post-buckling response of tapered composite plates under uni-axial compression", *Compos. Struct.*, **82**(2), 159-176. https://doi.org/10.1016/j.compstruct.2006.12.014

Ghosh, A. and Chakravorty, D. (2014), "Prediction of progressive failure behaviour of composite skewed hypar shells using finite element method", *J. Struct.*, Article ID **147578**, 1-8. http://dx.doi.org/10.1155/2014/147578

Ghosh, A. and Chakravorty, D. (2017), "Failure analysis of civil Engineering composite shell roofs", *Proce. Eng.*, **173**, 1642-1649. https://doi.org/10.1016/j.proeng.2016.12.258

Gohari, S., Golshan, A., Mostakhdemin, M., Mozafari, F. and Momenzadeh, A. (2012), "Failure strength of thin-walled cylindrical GFRP composite shell against static internal and external pressure for various volumetric fiber fraction", *Int. J. App. Phy. Math.*, **2**, 111-116.

Gohari, S., Sharifi, S., Vrcelj, Z. and Yahya, M.Y. (2015), "First ply failure prediction of an unsymmetrical laminated ellipsoidal woven GFRP composite shell with incorporated surface-bounded sensors and internally pressurized", *Compos.-Part B*, **77**, 502-518. https://doi.org/10.1016/j.compositesb.2015.03.058

Kam, T.Y., Sher, H.F., Chao, T.N. and Chang, R.R. (1996), "Predictions of deflection and first-ply failure load of thin laminated composite plates via the finite element approach", *Int. J. Solids Struct.*, **33**(3), 375-398. https://doi.org/10.1016/0020-7683(95)00042-9

Kelly, G. and Hallström, S. (2005), "Strength and failure mechanisms of composite laminates subject to localised transverse loading", *Compos. Struct.*, **69**(3), 301-314. https://doi.org/10.1016/j.compstruct.2004.07.008

Kober, M. and Kuhhorn, A. (2012), "Comparison of different failure criteria for fiber-reinforced plastics in terms of fracture curves for arbitrary stress combinations", *Compos. Sci. Tech.*, **72**, 1941-1951. https://doi.org/10.1016/j.compscitech.2012.08.007

Kumar, A., Chakrabarti, A. and Ketkar, M. (2013), "Analysis of laminated composite skew shells using higher order shear deformation theory", *Latin Am. J. Sol. Struct.*, **10**, 891-919. http://dx.doi.org/10.1590/S1679-78252013000500003

Lal, A., Singh, B.N. and Patel, D. (2012), "Stochastic nonlinear failure analysis of laminated composite plates under compressive transverse loading", *Compos. Struct.*, **94**(3), 1211-1223. https://doi.org/10.1016/j.compstruct.2011.11.018

Lee, C.S., Kim, J.H., Kim, S.K., Ryu, D.M. and Lee, J.M. (2015), "Initial and progressive failure analyses for composite laminates using Puck failure criterion and damage-coupled finite element method", *Compos. Struct.*, **121**, 406-419. https://doi.org/10.1016/j.compstruct.2014.11.011

Lopez, R.H., Luersen, M.A. and Cursi, E.S. (2009), "Optimization of laminated composites considering different failure criteria", *Compos.-Part B*, **40**, 731-740. https://doi.org/10.1016/j.compositesb.2009.05.007

Matthias, D.H. and Kröplin, B. (2012), "Finite element implementation of Puck's failure theory for fibre-reinforced composites under three-dimensional stress", *J. Compos. Mat.*, **46**(19-20), 2485-2513. https://doi.org/10.1177/0021998312451480

Nali, P. and Carrera, E. (2012), "A numerical assessment on two-dimensional failure criteria for composite layered structures", *Compos.-Part B*, **43**, 280-290. https://doi.org/10.1016/j.compositesb.2011.06.018

Neogi, S.D., Karmakar, A. and Chakravorty, D. (2011), "Impact response of simply supported skewed hypar shell roofs by finite element", *J. Reinf. Plast. Compos.*, **30**(21), 1795-1805. https://doi.org/10.1177/0731684411418865

Oterkus, E., Madenci, E., Weckner, O., Silling, S., Bogert, P. and Tessler, A. (2012), "Combined finite element and peridynamic analyses for predicting failure in a stiffened composite curved panel with a central slot", *Compos. Struct.*, **94**, 839-850. https://doi.org/10.1016/j.compstruct.2011.07.019

Owen, D.R.J. and Hinton, E. (1980), *Finite Elements in Plasticity: Theory and Practice*, Pineridge Press Limited, UK, Ch. 6, pp. 157-214.

Pal, P. and Ray, C. (2002), "Progressive failure analysis of laminated composite plates by finite element method", *J. Reinf. Plast. Compos.*, **21**(16), 1505-1513. https://doi.org/10.1177/0731684402021016488

Palazotto, A.N. and Dennis, S.T. (1992), *Nonlinear Analysis of Shell Structures*, AIAA Education Series, American Institute of Aeronautics and Astronautics (AIAA) Washington, DC, pp. 131-154.

Priyadharshani, S.A., Prasad, A.M. and Sundaravadivelu, R. (2017), "Analysis of GFRP stiffened composite plates with rectangular cutout", *Compos. Struct.*, **169**, 42-51. https://doi.org/10.1016/j.compstruct.2016.10.054

Prusty, B.G. (2005), "Progressive failure analysis of laminated unstiffened and stiffened composite panels", *J. Reinf. Plast. Compos.*, **24**(6), 633-642. https://doi.org/10.1177/0731684405045023

Qatu, M.S. and Leissa, A.W. (1991), "Vibration studies for laminated composite twisted cantilever plates", *Int. J. Mech. Sci.*, **33**(11), 927-940. https://doi.org/10.1016/0020-7403(91)90012-R

Reddy, J.N. (2004), *Mechanics of laminated composite plates and shells: Theory and Analysis*, CRC Press, Second Edition, Boca Raton, FL, USA.

Reddy, Y.S.N. and Reddy, J.N. (1992), "Linear and nonlinear failure analysis of composite laminates with transverse shear", *Compos. Sci. Tech.*, **44**, 227-255. https://doi.org/10.1016/0266-3538(92)90015-U

Reddy, Y.N.S., Moorthy, C.M.D. and Reddy, J.N. (1995), "Nonlinear progressive failure analysis of laminated composite plates", *Int. J. Nonlinear Mech.*, **30**, 629-649. https://doi.org/10.1016/0020-7462(94)00041-8

Reinoso, J. and Blázquez, A. (2016), "Application and finite element implementation of 7-parameter shell element for geometrically nonlinear analysis of layered CFRP composites", *Compos. Struct.*, **139**, 263-276. https://doi.org/10.1016/j.compstruct.2015.12.009

Reinoso, J., Catalanotti, G., Blázquez, A., Areias, P., Camanho, P.P. and París, F. (2017), "A consistent anisotropic damage model for laminated fiber-reinforced composites using the 3D-version of the Puck failure criterion", *Int. J. Sol. Struct.*, **126**, 37-53. https://doi.org/10.1016/j.ijsolstr.2017.07.023

Sahoo, S. and Chakravorty, D. (2004), "Finite element bending behaviour of composite hyperbolic paraboloidal shells with various edge conditions", *J. Str. Ana. Eng. Des.*, **39**(5), 499-513. https://doi.org/10.1243/0309324041896434

Singh, S.B. and Kumar, A. (1998), "Post buckling response and failure of symmetric laminates under in-plane shear", *Compos. Sci. Tech.*, **58**, 1949-1960. https://doi.org/10.1016/S0266-3538(98)00032-3

Singh, S.B., Kumar, A. and Iyengar, N.G.R. (1997), "Progressive failure of symmetrically laminated plates under uni-axial compression", *Struct. Eng. Mech., Int. J.*, **5**(4), 433-450. https://doi.org/10.12989/sem.1997.5.4.433

Singh, S.B., Kumar, A. and Iyengar, N.G.R. (1998a), "Progressive failure of symmetric laminates under in-plane shear: I-Positive shear", *Struct. Eng. Mech., Int. J.*, **6**(2), 143-159. https://doi.org/10.12989/sem.1998.6.2.143

Singh, S.B., Kumar, A. and Iyengar, N.G.R. (1998b), "Progressive failure of symmetric laminates under in-plane shear: II-Negative shear", *Struct. Eng. Mech., Int. J.*, **6**(7), 757-772. https://doi.org/10.12989/sem.1998.6.7.757

Soni, S.R. (1983), "A comparative study of failure envelops in composite laminates", *J. Reinf. Plast. Compos.*, **2**, 34-42. https://doi.org/10.1177/073168448300200104

Xiong, J., Ghosh, R., Ma, L., Vaziri, A., Wang, Y. and Wu, L. (2014), "Sandwich-walled cylindrical shells with lightweight metallic lattice truss cores and carbon fiber-reinforced composite face sheets", *Compos.-Part A*, **56**, 226-238. https://doi.org/10.1016/j.compositesa.2013.10.008

Xue, J., Ding, Y., Han, F. and Liu, R. (2013), "An extension of Karman-Donnell's theory for non-shallow, long cylindrical shells undergoing large deflection", *Europ. J. Mech. A/Solids*, **37**, 329-335. https://doi.org/10.1016/j.euromechsol.2012.08.004

Xue, J., Xia, F., Ye, J., Zhang, J., Chen, S., Xiong, Y., Tan, Z., Liu, R. and Yuan, H. (2017), "Multiscale studies on the nonlinear vibration of delaminated composite laminates-global vibration mode with micro buckles on the interfaces", *Sci. Reports*, **7** (1), 4468. https://doi.org/10.1038/s41598-017-04570-3

Xue, J., Jin, F., Zhang, J., Li, P., Xia, F., Xu, J., Liu, R. and Yuan, H. (2019), "Post-buckling induced delamination propagation of composite laminates with bi-nonlinear properties and anti-penetrating interaction effects", *Compos. Part B*, **166**, 148-161. https://doi.org/10.1016/j.compositesb.2018.11.082

Yang, Q.J. and Hayman, B. (2015), "Simplified ultimate strength analysis of compressed composite plates with linear material degradation", *Compos.-Part B*, **69**, 13-21. https://doi.org/10.1016/j.compositesb.2014.09.016

CC

List of notations

a, b	Length and width of hypar shell in plan
c	Rise of hypar shell
R_{xy}	Radii of cross curvature of the hypar shell
h	Shell thickness
X, Y, Z	Global coordinate axes
1, 2, 3	Local coordinate axes
N_x, N_y	In-plane normal force resultants
N_{xy}	In-plane shear force resultant
M_x, M_y	Moment resultants
M_{xy}	Torsional moment resultant
Q_x, Q_y	Transverse shear resultants
np	Number of ply
k_x, k_y, k_{xy}	Curvatures of the shell due to loading
γ_{xy} ,γ_{xz}, γ_{yz}	In-plane and transverse shear strains, respectively
ε_x, ε_y	In-plane strains along x and y axes of the shell
$\{\varepsilon_l\}$, $\{\varepsilon_{nl}\}$	Linear and nonlinear part of strain vectors, respectively
$[B]$, $[B']$	Linear and nonlinear strain displacement matrix, respectively
$[\bar{B}]$	Strain displacement matrix
z_k, z_{k-1}	Top and bottom distance of the k^{th} ply from mid-plane of a laminate
σ_1, σ_2	Normal stresses acting along 1 and 2 axes of a lamina, respectively
τ_{12}	Shear stress acting on 1-2 surface of a lamina
ε_1, ε_2	In-plane strains along 1 and 2 axes of a lamina, respectively
γ_{12}	In-plane shear strain acting on 1-2 surface of a lamina
E_{11}, E_{22}, E_{33}	Modulus of elasticity along the directions 1, 2 and 3
G_{12}, G_{13}, G_{23}	Shear modulus of a lamina in 1-2, 1-3, and 2-3 planes corresponding to the local axes of that lamina, respectively
ν_{ij}	Poisson's ratio
σ_{1T}^u, σ_{2T}^u	Ultimate normal tensile stresses along 1 and 2 direction, respectively
σ_{1C}^u, σ_{2C}^u	Ultimate normal compressive stresses along 1 and 2 direction, respectively
ε_{1T}^u, ε_{2T}^u	Ultimate normal tensile strains along 1 and 2 direction, respectively
ε_{1C}^u, ε_{2C}^u	Ultimate normal compressive strains along 1 and 2 direction, respectively
τ_{12}, τ_{13}, τ_{23}	Ultimate shear stress values in 1-2, 1-3, and 2-3 planes corresponding to the local axes of that lamina, respectively
γ_{12}, γ_{13}, γ_{23}	Ultimate shear strain values in 1-2, 1-3, and 2-3 planes corresponding to the local axes of that lamina, respectively
FL	Uniformly distributed first ply failure load values
$\overline{FL}$	Nondimensionalized uniformly distributed first ply failure load values = $(FL/E_{22})(a/h)^4$